TU Delft

Delft University of Technology

Document Version
Final published version

Licence
Dutch Copyright Act (Article 25fa)

Citation (APA)
Stam, M., Chen, H., Vogel, Y. B., Stavast, I., van Leeuwen, M., Ubbink, R. F., van Silfhout, N., van der Made, C. F. A., Houtepen, A. J., & More Authors (2026). Electrochemical Stability and Trap-State-Mediated Photoluminescence Modulation of InP-Based Quantum Dots. *Chemistry of Materials*, *38*(3), 1407-1414. https://doi.org/10.1021/acs.chemmater.5c02861

Important note
To cite this publication, please use the final published version (if applicable).
Please check the document version above.

Copyright
In case the licence states “Dutch Copyright Act (Article 25fa)”, this publication was made available Green Open Access via the TU Delft Institutional Repository pursuant to Dutch Copyright Act (Article 25fa, the Taverne amendment). This provision does not affect copyright ownership.
Unless copyright is transferred by contract or statute, it remains with the copyright holder.

Sharing and reuse
Other than for strictly personal use, it is not permitted to download, forward or distribute the text or part of it, without the consent of the author(s) and/or copyright holder(s), unless the work is under an open content license such as Creative Commons.

Takedown policy
Please contact us and provide details if you believe this document breaches copyrights.
We will remove access to the work immediately and investigate your claim.

This work is downloaded from Delft University of Technology.

CHEMISTRY OF MATERIALS

pubs.acs.org/cm

Article

Electrochemical Stability and Trap-State-Mediated Photoluminescence Modulation of InP-Based Quantum Dots

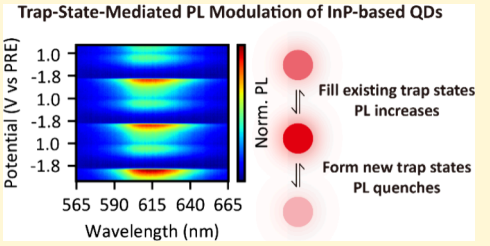
Maarten Stam,[§] Hua Chen,[§] Yan B. Vogel, Irene Stavast, Mourijn van Leeuwen, Reinout F. Ubbink, Niels van Silfhout, Colin F. A. van der Made, Luca Giordano, Pieter Schiettecatte, Zeger Hens, and Arjan J. Houtepen*

Cite This: *Chem. Mater.* 2026, 38, 1407−1414

Read Online

ACCESS | Metrics & More | Article Recommendations | Supporting Information

ABSTRACT: Indium phosphide (InP) quantum dots (QDs) are promising heavy-metal-free materials for optoelectronics, but their redox stability, trap-state landscape, and charge carrier dynamics are not well understood. Here we investigate InP and InP/ZnSe/ZnS QD films with different ligands by using spectroelectrochemistry. For both core-only and core/shell/shell QD films, the absorption spectra remain unchanged during charging, indicating that injected charges do not populate the conduction or valence bands. InP/ZnSe/ZnS QD films with original ligands exhibit reversible photoluminescence (PL) modulation: an increase at modest cathodic potentials, followed by quenching at more negative potentials. Solid-state ligand exchange using ethylenediamine (2DA) and sodium sulfide (Na_2S) enhances conductivity and induces stronger PL changes at both cathodic and anodic potentials. These results are in line with the population of electron traps at modest cathodic potentials (i.e., near the midbandgap), suppressing nonradiative recombination and increasing the PL. At more negative potentials, electrochemical reactions of surface species result in new trap states quenching the PL. Our findings provide insights into the stability and trap-state-mediated carrier dynamics during electrochemical charging of InP-based QDs.



INTRODUCTION

Quantum dots (QDs) are luminescent materials with size-dependent optical properties, high photoluminescence quantum yields (PLQYs), and narrow emission. These properties make QDs appealing for numerous optoelectronic applications such as photodetectors, light-emitting diodes (LEDs), and lasers.[1−7] The toxic nature of Cd chalcogenide and Pb halide perovskite QD materials has directed research toward InP-based QDs that are compliant with the Restriction of Hazardous Substances (RoHS) directive (Directive 2011/65/EU of the European Parliament).

Currently, InP-based QDs can be synthesized with near-unity PLQYs[8−10] and narrow emission.[11,12] Efficient LEDs have been fabricated with these QDs.[8,12−14] During the operation of LEDs, electrons and holes are injected into the QDs, which may cause reduction or oxidation reactions, inducing stability issues. In fact, it has been shown in bulk semiconductors that charge carrier injections can lead to charge-compensating defects.[15−17] Electrochemical measurements offer a promising approach to probe the stability of InP-based QDs during charge injection, as charges are continuously supplied throughout the measurement. This continuous charge injection accentuates the effects, increasing the likelihood of detecting stability changes compared to methods such as photoexcitation, where charge carriers are transient.

The effects of charge injection into QDs have been studied both computationally and experimentally. Theoretical studies of Cd-based QDs show that injection of more than one electron can lead to the formation of trap states, even in completely passivated QDs, and that the absence of ligands can facilitate the reduction of Cd atoms on the surface.[18,19] In experimental work, injection of charge into the conduction band (CB) for CdSe/CdS/ZnS QD films is reported,[20,21] where the protective ZnS shell is necessary to remove shallow trap states that are suspected to give rise to enhanced hole trapping once these traps are filled with electrons electrochemically.[22] Moreover, using electrochemically stable ligands, such as amines instead of cadmium carboxylates, proved to be essential to maintain high electroluminescence in Cd-based QD-LEDs.[23]

On ZnO and PbS QD films, it is possible to reversibly inject and extract electrons into and/or from the CB without degrading the QD films.[24−29] On InP-based QDs, our previous theoretical study revealed that undercoordinated In atoms at the surface of core-only InP QDs are responsible for trap-state formation when negative charges are injected, which can be prevented by growing a protective ZnSe layer around these

Received: October 25, 2025
Revised: January 15, 2026
Accepted: January 16, 2026
Published: January 28, 2026



Downloaded via TU DELFT on March 26, 2026 at 16:01:11 (UTC).
See https://pubs.acs.org/sharingguidelines for options on how to legitimately share published articles.

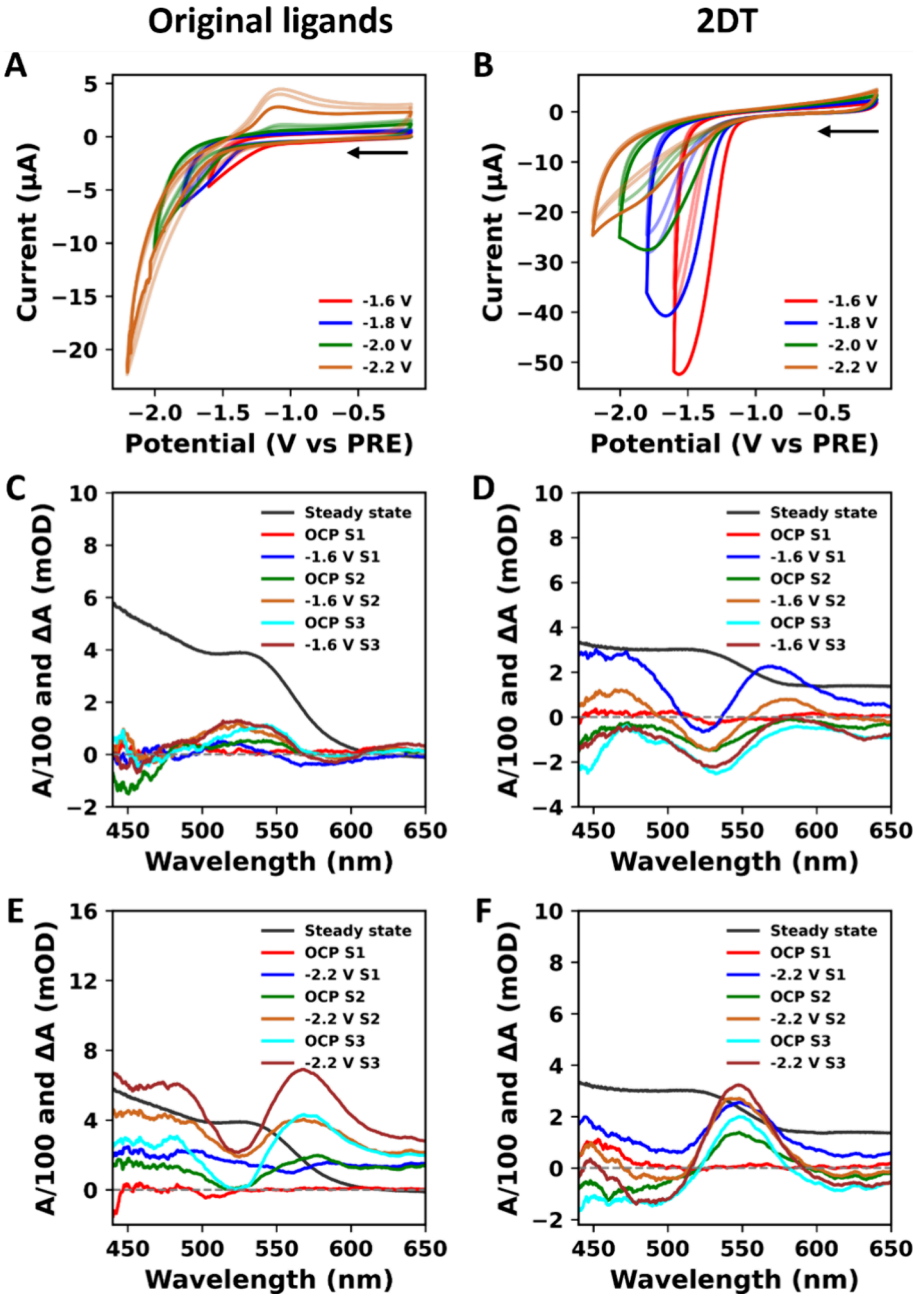


Figure 1. Spectroelectrochemical measurements on InP QD films. Cyclic voltammograms starting at the OCP to increasingly negative potentials for InP QD films with (A) original ligands (chloride and oleylamine) and (B) 2DT as ligands recorded at a scan rate of 50 mV/s in 0.1 M $TBAPF_6$ in acetonitrile as the electrolyte. Each cyclic voltammogram contains three consecutive scans where the first scan is indicated in a dark shade and the second and third scans are indicated in a lighter shade of the same color. The scan direction for each cyclic voltammogram is indicated by the black arrow. The absorption and differential absorption spectra at the OCP and the most negative potential for three consecutive scans (S1−S3) are displayed in panels C and E for films with the original ligands and in panels D and F for films with the 2DT ligands.

cores.[30] These findings seem to line up with experimental work on bulk (100)-oriented InP electrodes where metallic In is formed at negative potentials[31] and with the reported works on InP-based QDs in dispersion where charging of InP/ZnSe/ZnS is claimed.[32,33] However, knowledge of InP-based QD films, which resemble more closely QDs in devices, is lacking.

In this work, we study InP core-only and InP/ZnSe/ZnS core/shell/shell QD films using spectroelectrochemistry. We apply a potential on the QD film and monitor simultaneously the electrochemical current and changes in absorbance and PL. In cyclic voltammograms recorded on InP and InP/ZnSe/ZnS QD films, there is no significant change in the absorption spectrum, indicating that the injected carriers do not populate the conduction or valence bands. However, we do observe a reversible PL modulation on InP/ZnSe/ZnS QD films. With the original ligands, PL increases and then decreases when a negative potential is applied and only recovers fully when the potential is scanned to positive values. We performed a solid-state ligand exchange on core/shell/shell QD films to improve conductivity using either 1,2-ethanedithiol (2DT), ethylenediamine (2DA), or sodium sulfide (Na_2S),[34] resulting in more pronounced PL changes. PL modulation in the absence of charge carriers in the CB or valence band (VB) suggests trap-state-mediated processes. At a cathodic potential between the

https://doi.org/10.1021/acs.chemmater.5c02861
Chem. Mater. 2026, 38, 1407−1414

open circuit potential (OCP) and −1.3 V, electrons populate preexisting traps, suppressing nonradiative recombination, and at a potential of more negative than −1.3 V or more positive than 0.5 V, electrochemical reactions of ligands or surface ions generate new trap states that quench PL.

RESULTS AND DISCUSSION

Core-Only InP QD Films

The core-only InP QDs are synthesized using $InCl_3$, $ZnCl_2$, and tris(diethylamino)phosphine (see the Experimental Section for details).[35] The synthesized QDs have a cation-rich surface where the ratio of In and Zn to P is 1.09.[36] These QDs have a 1S absorption peak at approximately 530 nm, and the PL spectrum is dominated by trap-state emission (Figure S1), which is common for as-synthesized InP QDs.[10,37−40] The QD films were drop-cast onto fluorine-doped tin oxide (FTO) substrates. We used them as the working electrode in our spectroelectrochemical measurements (further details in the Experimental Section). In a typical measurement, we change the potential linearly from open circuit potential (OCP) to cathodic vertex potential and back to the OCP at a scan rate of 50 mV/s, using 0.1 M $TBAPF_6$ in acetonitrile as the electrolyte. The potential in this work is referred to a silver pseudoreference electrode (PRE) that is calibrated using a ferrocene/ferrocenium redox couple (Figure S2).

We first performed cyclic voltammetry (CV) at increasingly cathodic vertex potentials (−1.6, −1.8, −2.0, and −2.2 V) on InP QD films with the original ligands (chloride/oleylamine)[41] to determine the stable electrochemical window, i.e., the potential window where the QDs do not undergo irreversible electrochemical reactions (Figure 1A). We observe an irreversible cathodic current at potentials below −1.3 V of a magnitude comparable to that of a bare (i.e., without QDs) FTO electrode (see Figure S3 for the cyclic voltammogram on a bare FTO). This indicates that the electrochemical reaction does not involve QDs and is likely due to O_2 reduction.[42] For vertices beyond −2.0 V, an anodic peak near −1.1 V emerges on the backward scan, absent in FTO, indicating the presence of reduction of QD ligands or surface atoms on the forward scan, which are subsequently oxidized when scanned back.

The original long-chain ligands would impede the charge transfer between QDs, and thus, electrochemical doping of the QDs could not be observed. Therefore, we performed a solid-state ligand exchange with a bidentate ligand (2DT) to reduce the distance between the InP QDs to enhance conductivity.[34] The cyclic voltammograms (Figure 1B) exhibit larger irreversible cathodic currents than those of the QD films with the native ligands (Figure 1A) and the bare FTO electrode. This indicates the presence of an electrochemical reaction on the QDs and confirms our hypothesis that poor film conductivity is due to the native ligands.

The observation that subsequent scans have smaller cathodic currents is consistent with an irreversible cathodic reaction that consumes the species present. However, from the current data alone, we cannot determine the nature of this electrochemical reaction. Therefore, we next looked into changes in the absorption spectrum to gain insights into the nature of this reaction. Panels C and E of Figure 1 show the differential spectra for the core-only QD film with the chloride/oleylamine ligands at the OCP and at −1.6 and −2.2 V. At both cathodic potentials, the changes in absorbance are very small (∼1% of the 1S peak absorbance), indicating negligible degradation of QDs happened. There is, however, a small and irreversible red-shift that we attribute to a Stark effect induced by surface charges, as also observed for electrochemically charged CdSe and CdTe QD films.[22,43−45] In addition, at −2.2 V there is an increase in absorbance over the full wavelength range, reminiscent of enhanced light scattering. This scattering could be due to expansion of the film or an increase in dielectric constants, for instance, caused by the electrodeposition of metal domains.[46] Similar minimal changes in absorbance are seen in measurements with cathodic vertex potentials of −1.8 and −2.0 V (Figure S4). XPS of the core-only InP QD films before and after the measurement shows no obvious shift in the In 3d, Zn 2p, and P 2p spectra, indicating that there is no significant reduction of In^{3+} and Zn^{2+} in the QD film (Figure S5). We do observe an increase in oxidized phosphorus. However, it is unlikely that phosphorus is oxidized during cathodic charging. Therefore, we ascribe it to possible air exposure during sample preparation for XPS measurements. For QD films with 2DT ligands, as shown in panels D and F of Figure 1, a similar red-shift has been observed when the film is only scanned to −1.6 V, indicating higher conductivity compared to that of QD films with the original ligands. Overall, the differential absorbance measurements suggest negligible redox reactions of InP core-only QDs and no population into CB.

Core/Shell/Shell InP/ZnSe/ZnS QD Films

We gain further insights into the nature of electrochemical reactions by monitoring the PL during electrochemical charging. We performed spectroelectrochemical experiments on InP QDs shelled with approximately seven monolayers of ZnSe and three monolayers of ZnS (details of the synthesis in the Experimental Section), because their increased luminescence allows the PL to be probed *in situ*. We expect that InP/ZnSe/ZnS QDs are more electrochemically stable than core-only InP QDs because the standard reduction potential (in an aqueous electrolyte) for In^{3+}, −0.34 V versus NHE, is more positive than for Zn^{2+}, −0.76 V versus NHE.[47−49] The protective role of Zn on the outer layer of InP/ZnSe QDs is also described in our previous computational work.[30] The QD dispersion has a 1S absorbance and emission at 580 and 611 nm and a PLQY of 63% (Figure S6). The InP/ZnSe/ZnS QDs have a mixture of oleylamine, zinc oleate, and zinc acetate as capping ligands on their surface.[50] We prepared the InP/ZnSe/ZnS films in the same manner as that for the core-only QD films.

Figure 2 shows three CV scans of the current and PL monitored at 615 nm and the corresponding 2D PL plots, for a cathodic scan (Figure 2A,B, OCP to −1.8 V and back), anodic scan (Figure 2C,D, OCP to 1.0 V and back), and the complete electrochemical window (Figure 2E,F, OCP to −1.8 V, then to 1.0 V and back to the OCP). At potentials below −1.0 V (Figure 2A,B), we observe an irreversible cathodic current like that with the core-only QDs. There is a slight increase in PL followed by a sharp decrease at −1.0 V, which recovers but not completely on the reverse scan. The electrochemical and optical signals are reproducible in subsequent scans but with lower intensity due to the partial irreversibility of the reaction. At anodic potentials (Figure 2C,D), we observe a small irreversible current that is about 10 times lower than the cathodic current and a completely reversible decrease (of about 10% of the original value) in PL. The PL is also completely reversible when the potential is scanned cathodi-

https://doi.org/10.1021/acs.chemmater.5c02861
Chem. Mater. 2026, 38, 1407−1414

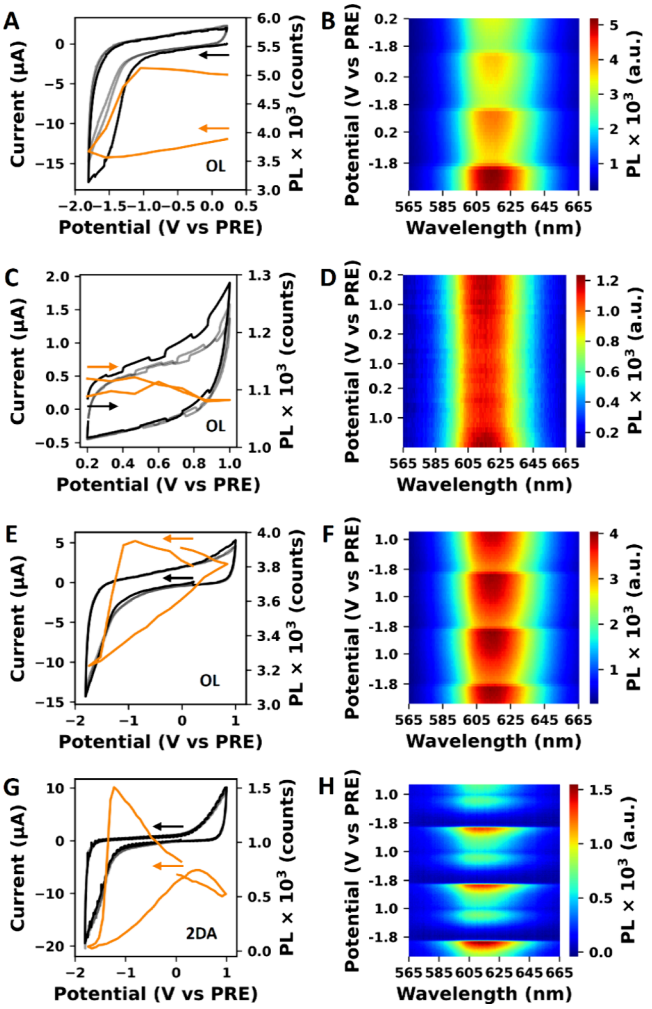


Figure 2. Spectroelectrochemical measurements on InP/ZnSe/ZnS QD films. Cyclic voltammograms (black) measured between (A) OCP and −1.8 V, (C) OCP and 1.0 V, and (E) −1.8 and 1.0 V of samples with original ligands and (G) −1.8 and 1.0 V of samples ligand exchanged with 2DA. All of the cyclic voltammograms were recorded at a scan rate of 100 mV/s starting at 0.2 V in 0.1 M $TBAPF_6$ in acetonitrile as the electrolyte; the second and third scans are colored gray. The black arrow indicates the starting point and the direction of the cyclic voltammogram, and the orange arrow indicates the starting point and the direction of the PL during the cyclic voltammogram. The PL intensity over one scan is colored orange. (B, D, F, and H) Corresponding two-dimensional plots over the entire cyclic voltammograms.

cally to −1.8 V and then anodically to 1.0 V (Figure 2E,F) or first anodically and then cathodically (Figure S7). Auger recombination is often considered a key mechanism for PL quenching during electrochemical charging. In our steady-state measurements, we do not observe any reversible absorption bleaching (Figure S8), suggesting a very low CB or VB population, which is at most within the noise of the SEC measurements. While this seems to suggest that Auger recombination is not the main cause of PL quenching, it should be considered that photogenerated excitons can diffuse over many QDs during their lifetime and potentially find an excess carrier even at a low concentration of injected charges and undergo Auger recombination. We have previously found that carrier densities of 0.01 exciton per QD can already induce Auger recombination in conductive QD films.[51] Therefore, we cannot rule out Auger recombination as the cause of PL quenching.

Similarly to core-only QDs, the core/shell/shell QD films exchanged with shorter ligands (2DT, 2DA, and Na_2S) show increased electrical and optical signals (Figure 2 G,H and Figure S9). Although film conductivity is improved by solid-state ligand exchange, there is no obvious change in the absorption spectrum of InP/ZnSe/ZnS QD films, indicating that injected carriers do not persist in the conduction or valence bands (Figure S10). The observation that PL quenching begins at similar negative potentials across different films (Figure 3 and Table S1) indicates that the underlying

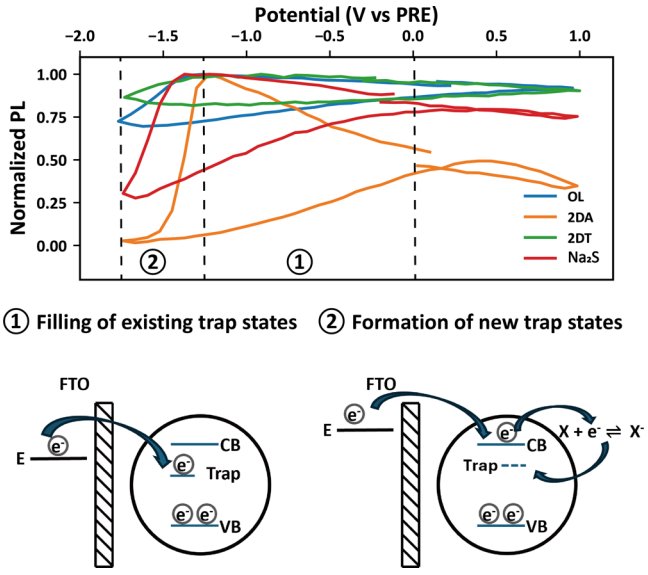


Figure 3. Potential-dependent normalized PL response of InP/ZnSe/ZnS QD films with original ligands, 2DA, 2DT, and Na_2S ligands. Two regimes are observed: (1) filling of existing trap states (OCP to −1.3 V vs PRE), leading to enhanced PL, and (2) formation of new trap states (less than −1.3 V vs PRE), resulting in PL quenching.

energy levels are not significantly shifted. This suggests that the electronic structure of the quantum dots, particularly the conduction band edge, remains largely unaffected by ligand exchange or other modifications. Instead of energy-level shifts, the magnitude of PL changes appears to scale with the increased current flow, which reflects enhanced charge carrier mobility in the films. Higher mobility facilitates greater charge injection into the system, leading to more pronounced PL quenching under both cathodic and anodic bias. When scanning from the OCP cathodically to approximately −1.3 V, the PL intensity initially increases. As illustrated in Figure 3, we attribute this to the filling of preexisting electron trap states, which reduces nonradiative recombination pathways. The enhanced PL therefore reflects competition between electron and hole trapping, with electron trapping occurring more efficiently, similar to the trends reported for CdTe QDs.[43] At potentials more negative than −1.3 V and more positive than 0.5 V, the PL decreases sharply. We assign this to reduction or oxidation of surface complexes (ligands or surface ions), which introduces new trap states that quench emission. Importantly, this process is chemically reversible. The PL recovers upon reversal of the potential sweep, indicating that these surface reactions do not irreversibly degrade the QDs.

https://doi.org/10.1021/acs.chemmater.5c02861
Chem. Mater. 2026, 38, 1407−1414

CONCLUSIONS

During electrochemical doping of InP and InP/ZnSe/ZnS QD films, there is no obvious change in the absorption spectrum, indicating that injected carriers do not persist in the conduction or valence bands. The potential-dependent PL modulation is observed on InP/ZnSe/ZnS QDs, and solid-state ligand exchange with 2DA and Na_2S induces a stronger PL change due to the increase in film conductivity. We propose that at potentials between OCP and −1.3 V electrons populate trap states that already exist in the bandgap and thus increase the PLQY, while at potentials of more negative than −1.3 V or more positive than 0.5 V electrochemical reactions of ligands or surface ions occur that reduce the PLQY. These reactions are chemically reversible, by scanning the potential in the opposite direction.

Our work reveals that while the PL of InP-based quantum dot films can be modulated electrochemically, stable and reversible charging into the band-edge states is hindered by surface redox reactions that consume injected carriers. This indicates that an electrochemically stable surface is required to achieve stable electrochemical doping of InP-based QDs. Future efforts may focus on surface chemistries that suppress parasitic surface reactions while preserving the conductivity. Additionally, efficient QD-LEDs have been successfully fabricated using InP-based QDs, suggesting that achieving stable electrochemical charging is possible. Rather than abandoning electrochemical approaches, our work offers an initial step toward understanding how surface chemistry influences charge injection stability in InP-based QD solids.

EXPERIMENTAL SECTION

Materials

The following materials were purchased from Merck Sigma: fluorescein (≥95.0%), $InCl_3$ (99.999%), $ZnCl_2$ (>98%), tris-(diethylamino)phosphine (97%), triethylamine (≥99%), zinc oxide (99.999%), 1,2-ethanedithiol (≥98.0%), ethylenediamine (≥99%), sodium sulfide (≥99%), and tetrabutylammonium hexafluorophosphate for the electrolyte ($TBAPF_6$) (≥99.0%). Anhydrous toluene (99.8%), selenium powder 200 mesh (99.999%), oleic acid (technical 90%), trifluoroacetic acid (99%), trifluoroacetic anhydride (>99%), and 1-octadecene (technical 90%) were acquired from Alfa Aesar. Tri-*n*-octylphosphine (>97%) and sulfur powder (99.999%) were purchased from Strem Chemicals. NaOH pellets (98.5%), oleylamine (80−90%), calcium(II) hydride (93%), and zinc acetate (99%) were purchased from Acros Organics. Anhydrous ethanol (>99.5%) tetrabutylammonium hexafluorophosphate for synthesis (98%), and anhydrous acetonitrile (≥99.95%) were purchased from VWR. Methanol was obtained from Fisher Chemicals. 2-Propanol (99.7%) was purchased from Chem-Lab Analytical. Ar (6 N) was purchased from Linde. Fluorine-doped tin oxide (FTO) on glass slides (1.1 mm thick, 12−15 Ω/square) was purchased from MSE Supplies. Oleylamine and 1-octadecene were dried over calcium(II) hydride, degassed via a vacuum distillation, and stored over molecular sieves in a nitrogen-filled glovebox prior to use. All other chemicals were used without further purification.

Transamination of Tris(diethylamino)phosphine

Transamination of tris(diethylamino)phosphine occurs in the presence of 3 equiv of oleylamine at 120−140 °C until the solution turns pale yellow in a nitrogen-filled glovebox. Then, 0.25 mL (0.91 mmol) of tris(diethylamino)phosphine is added to 1 mL (3.03 mmol) of oleylamine. Afterward, while the mixture is being stirred, the temperature is increased to 120−140 °C. The evaporated diethylamine gas is removed via a continuous flushing of the glovebox.

Zinc(II) Oleate Synthesis

We used a procedure based on the synthesis of lead(II) oleate by Hendricks et al. that was adapted by Dhaene et al. for the production of zinc oleate.[52,53] More specifically, 14.64 g (180 mmol) of zinc oxide was mixed in 80 mL (1.532 mol) of acetonitrile, and while the mixture was being cooled in an ice bath, 25.44 mL (180 mmol) of trifluoroacetic anhydride and 2.76 mL (36 mmol) of trifluoroacetic acid were added. The solution was stirred overnight, and a clear and colorless solution was obtained upon reaching room temperature. This zinc trifluoroacetate solution was added to a mixture of 102.2 g (361.8 mmol) of oleic acid, 41.16 g (406.8 mmol) of triethylamine, and 720 mL (2.351 mol) of 2-propanol, resulting in the formation of a white precipitate. The resulting mixture was stirred, and dissolution of the product occurred at reflux temperature. The flask is cooled to room temperature over a period of 2 h, followed by freezing to −20 °C overnight. The resulting white crystals were filtered off and washed with cold methanol. The synthesized powder was dried under vacuum, and a chemical yield of 95 ± 2% was obtained.

Tri-*n*-octylphosphine Selenide

A 2.24 M TOP-Se solution was prepared by dissolving 6.196 g (78.5 mmol) of selenium powder into 35 mL (78.5 mmol) of TOP at 90 °C for 1 h in a nitrogen-filled glovebox. Afterward, the mixture was kept for 30 min at 110 °C, upon which the mixture turned yellow. This TOP-Se solution was pushed through a 0.2 μm PTFE filter (VWR), and extra drops of TOP were added at 90 °C using a Pasteur pipet until the yellow color disappeared.

Tri-*n*-octylphospine Sulfide

A 2.24 M TOP-S solution was prepared by dissolving 2.517 g (78.5 mmol) of sulfur powder in 35 mL (78.5 mmol) of TOP at 90 °C for 1 h in a nitrogen-filled glovebox. Afterward, the hot solution was pushed through a 0.2 μm PTFE filter (VWR).

Synthesis of Core-Only InP QDs

The procedure is based on the method previously published by Tessier et al.[35] First, 100 mg (0.45 mmol) of indium(III) chloride and 300 mg (2.20 mmol) of zinc(II) chloride were mixed in 3 mL (9.10 mmol) of anhydrous oleylamine in a 25 mL flask. The mixture was stirred and degassed at 120 °C for 1 h and then heated to 180 °C under an inert atmosphere. Upon reaching 180 °C, 0.50 mL (1.83 mmol) of tris(diethylamino)phosphine, transaminated with 2 mL (6.07 mmol) of anhydrous oleylamine, was quickly injected in the reaction mixture described above, and the InP nanocrystal synthesis proceeded for 30 min. The synthesized InP QDs were purified by using anhydrous ethanol.

Synthesis of Core/Shell/Shell InP/ZnSe/ZnS QDs

In a 25 mL three-neck flask, 100 mg (0.45 mmol) of indium(III) chloride as indium raw material and 300 mg (2.20 mmol) of zinc(II) chloride as zinc raw material were mixed in 3 mL (9.10 mmol) of anhydrous oleylamine. The mixture was stirred and degassed at 120 °C for 1 h and then heated to 180 °C under an inert atmosphere. Upon reaching 180 °C, 0.50 mL (1.83 mmol) of tris(diethylamino)-phosphine, transaminated with 2 mL (6.07 mmol) of anhydrous oleylamine, was quickly injected into the reaction mixture described above, and the InP nanocrystal synthesis proceeded. After 30 min, the dispersion was cooled to 120 °C, and 120 mg (0.31 mmol) of tetrabutylammonium hexafluorophosphate, 0.3 mL (16.65 mmol) of water, and 2 g (3.18 mmol) of zinc(II) oleate mixed in 2 mL (6.07 mmol) of oleylamine and 4 mL (12.50 mmol) of 1-octadecene were added as a surface treatment prior to ZnSe shell growth. Subsequently, the mixture was stirred and degassed for 1 h. Afterward, 1.6 mL of a stoichiometric TOP-Se (2.24 M) solution was injected, and the temperature was increased to 330 °C. At this temperature, the shell growth continued for 45 min. Subsequent to the ZnSe shell growth, the reaction mixture was cooled to 120 °C, after which 400 mg (2.21 mmol) of zinc(II) acetate was added, and the mixture was stirred and degassed for 1 h. Consecutively, 1 mL of a stoichiometric TOP-S (2.24 M) solution was injected, and the temperature was increased to 300 °C. After ZnS shell growth for 1 h, the reaction was

https://doi.org/10.1021/acs.chemmater.5c02861
Chem. Mater. 2026, 38, 1407−1414

stopped by cooling the mixture to room temperature. InP/ZnSe/ZnS QDs were then precipitated once using anhydrous ethanol, redispersed in anhydrous toluene, and stored in a N_2-filled glovebox.

QD Film Preparation and Ligand Exchange

The QD films were prepared by drop-casting the QD dispersion (30 μL) on the FTO substrate and letting the solvent evaporate at room temperature. For ligand exchange, the dry films were submerged in a 0.1 M solution of the preferred ligand (2DT, 2DA, or Na_2S) in anhydrous acetonitrile for 30 s and afterward rinsed with anhydrous acetonitrile.

Spectroelectrochemical Measurements

An Autolab PGSTAT128N potentiostat operated with NOVA 2.1 software is used for the spectroelectrochemical measurement. The electrochemical cell is composed of a three-electrode setup with a platinum sheet as the counter electrode, a silver wire as the pseudoreference electrode, and the QD film on FTO as the working electrode. FTO was chosen as the conductive transparent substrate for its wider stability window compared to ITO. All experiments were performed inside a N_2-filled glovebox. A 0.1 M solution of $TBAPF_6$ in anhydrous acetonitrile was purged with argon gas (99.999%) for 15 min and used as the electrolyte. The optical spectra were recorded with a fiber-coupled spectrophotometer (Ocean Optics USB2000), and the white light for absorbance and blue light for photoluminescence measurements were generated by an Ocean Optics deuterium DH-2000 lamp and a 4.5 mW collimated laser diode from Thorlabs at a wavelength of 405 nm, respectively.

Optical Characterization

A PerkinElmer Lambda 365 spectrometer was used to record the UV−vis absorption spectra. An Edinburgh Instruments FLS980 spectrofluorometer with double grating monochromators for both excitation and emission paths and a 450 W xenon lamp was used as an excitation source. PLQY values were obtained with respect to the fluorescein reference dye in 0.1 M NaOH in water at room temperature. The PLQY was calculated using the following equation.

$$\mathrm{PLQY} = \mathrm{PLQY}_{\mathrm{fluorescein}} \times \frac{I^{\mathrm{PL}}_{\mathrm{QD\ dispersion}} f_{\mathrm{fluorescein}}}{I^{\mathrm{PL}}_{\mathrm{fluorescein}} f_{\mathrm{QD\ dispersion}}} \times \left(\frac{n_{\mathrm{toluene}}}{n_{\mathrm{water}}}\right)^2$$

where $\mathrm{PLQY}_{\mathrm{fluorescein}}$ is set to 92% for an excitation wavelength of 465 nm,[54] I^{PL} is the intensity of the PL signal of either the fluorescein solution or the QD dispersion, n is the refractive index of toluene or water at 465 nm (1.497 and 1.333), and f is the fraction of absorbed light for the fluorescein or toluene solution, calculated as $f = 10^{-\mathrm{OD}}$, where OD is the optical density of the fluorescein or QD dispersion at 465 nm.

X-ray Photoelectron Spectroscopy (XPS)

Samples are drop-cast on thin conductive substrates. XPS measurements were performed in ultrahigh vacuum with a ThermoFisher K-Alpha instrument equipped with an Al Kα source that radiates with an energy of 1486 eV. An Ar flood gun was used during the measurements to prevent charging of the films. All of the spectra were charge-corrected to the C−C peak in the C 1s spectrum that is set to 284.8 eV.

■ ASSOCIATED CONTENT

Supporting Information

The Supporting Information is available free of charge at https://pubs.acs.org/doi/10.1021/acs.chemmater.5c02861.

Optical characterization of InP core-only and InP/ZnSe/ZnS core/shell/shell dispersion in toluene, a cyclic voltammogram of ferrocene for calibration of the Ag pseudoreference (PRE) electrode, a cyclic voltammogram of a bare FTO substrate, steady-state and differential absorbance spectra for both InP core-only and InP/ZnSe/ZnS QD films, XPS spectra of an InP QD film, a cyclic voltammogram and 2D plot of PL for an InP/ZnSe/ZnS QD film, and a table containing the onset potential for the PL decrease for InP/ZnSe/ZnS QD films with different ligands (PDF)

■ AUTHOR INFORMATION

Corresponding Author

Arjan J. Houtepen − *Optoelectronic Materials Section, Faculty of Applied Sciences, Delft University of Technology, 2629 HZ Delft, The Netherlands;* orcid.org/0000-0001-8328-443X; Email: A.J.Houtepen@tudelft.nl

Authors

Maarten Stam − *Optoelectronic Materials Section, Faculty of Applied Sciences, Delft University of Technology, 2629 HZ Delft, The Netherlands*

Hua Chen − *Optoelectronic Materials Section, Faculty of Applied Sciences, Delft University of Technology, 2629 HZ Delft, The Netherlands;* orcid.org/0009-0002-3391-9403

Yan B. Vogel − *Optoelectronic Materials Section, Faculty of Applied Sciences, Delft University of Technology, 2629 HZ Delft, The Netherlands;* orcid.org/0000-0003-1975-7292

Irene Stavast − *Optoelectronic Materials Section, Faculty of Applied Sciences, Delft University of Technology, 2629 HZ Delft, The Netherlands*

Mourijn van Leeuwen − *Optoelectronic Materials Section, Faculty of Applied Sciences, Delft University of Technology, 2629 HZ Delft, The Netherlands*

Reinout F. Ubbink − *Optoelectronic Materials Section, Faculty of Applied Sciences, Delft University of Technology, 2629 HZ Delft, The Netherlands;* orcid.org/0000-0001-7714-5097

Niels van Silfhout − *Optoelectronic Materials Section, Faculty of Applied Sciences, Delft University of Technology, 2629 HZ Delft, The Netherlands*

Colin F. A. van der Made − *Optoelectronic Materials Section, Faculty of Applied Sciences, Delft University of Technology, 2629 HZ Delft, The Netherlands*

Luca Giordano − *Physics and Chemistry of Nanostructures, Department of Chemistry, Ghent University, 9000 Ghent, Belgium*

Pieter Schiettecatte − *Physics and Chemistry of Nanostructures, Department of Chemistry, Ghent University, 9000 Ghent, Belgium*

Zeger Hens − *Physics and Chemistry of Nanostructures, Department of Chemistry, Ghent University, 9000 Ghent, Belgium;* orcid.org/0000-0002-7041-3375

Complete contact information is available at: https://pubs.acs.org/10.1021/acs.chemmater.5c02861

Author Contributions

[§]M.S. and H.C. contributed equally to this work.

Funding

This publication is part of the project Quantum Dots for Advanced Lighting Applications (QUALITy) with Project 17188 of the Open Technology Programme, which is (partly) financed by the Dutch Research Council (NWO). Z.H. acknowledges the FWO-Vlaanderen (Projects G0B2921N and G0C5723N) and Ghent University (Grant 01G02124) for research funding. P.S. acknowledges FWO-Vlaanderen for

funding (Grant 12A9123N). H.C. thanks the China Scholarship Council for funding (File 202206120047).

Notes

The authors declare no competing financial interest.

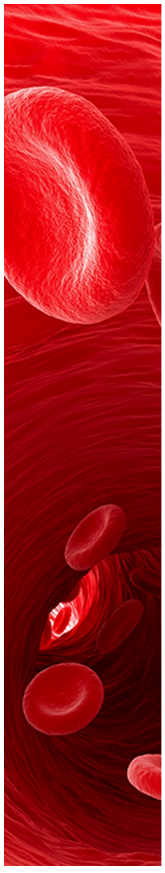
■ ACKNOWLEDGMENTS

The authors thank Bahiya Ibrahim, Jos Thieme, John Suijkerbuijk, and Wiel Evers for technical assistance with the spectroelectrochemical measurements.

■ REFERENCES

(1) Almeida, G.; Ubbink, R. F.; Stam, M.; du Fossé, I.; Houtepen, A. J. InP colloidal quantum dots for visible and near-infrared photonics. *Nature Reviews Materials* **2023**, *8* (11), 742−758.
(2) Wu, Z.; Liu, P.; Zhang, W.; Wang, K.; Sun, X. W. Development of InP Quantum Dot-Based Light-Emitting Diodes. *ACS Energy Letters* **2020**, *5* (4), 1095−1106.
(3) Park, Y.-S.; Roh, J.; Diroll, B. T.; Schaller, R. D.; Klimov, V. I. Colloidal quantum dot lasers. *Nature Reviews Materials* **2021**, *6* (5), 382−401.
(4) Coe-Sullivan, S.; Liu, W.; Allen, P.; Steckel, J. S. Quantum Dots for LED Downconversion in Display Applications. *ECS Journal of Solid State Science and Technology* **2013**, *2* (2), R3026.
(5) Talapin, D. V.; Steckel, J. Quantum dot light-emitting devices. *MRS Bull.* **2013**, *38* (9), 685−691.
(6) Geiregat, P.; Houtepen, A. J.; Sagar, L. K.; Infante, I.; Zapata, F.; Grigel, V.; Allan, G.; Delerue, C.; Van Thourhout, D.; Hens, Z. Continuous-wave infrared optical gain and amplified spontaneous emission at ultralow threshold by colloidal HgTe quantum dots. *Nat. Mater.* **2018**, *17* (1), 35−42.
(7) Geuchies, J. J.; Brynjarsson, B.; Grimaldi, G.; Gudjonsdottir, S.; van der Stam, W.; Evers, W. H.; Houtepen, A. J. Quantitative Electrochemical Control over Optical Gain in Quantum-Dot Solids. *ACS Nano* **2021**, *15* (1), 377−386.
(8) Won, Y.-H.; Cho, O.; Kim, T.; Chung, D.-Y.; Kim, T.; Chung, H.; Jang, H.; Lee, J.; Kim, D.; Jang, E. Highly efficient and stable InP/ZnSe/ZnS quantum dot light-emitting diodes. *Nature* **2019**, *575* (7784), 634−638.
(9) Van Avermaet, H.; Schiettecatte, P.; Hinz, S.; Giordano, L.; Ferrari, F.; Nayral, C.; Delpech, F.; Maultzsch, J.; Lange, H.; Hens, Z. Full-Spectrum InP-Based Quantum Dots with Near-Unity Photoluminescence Quantum Efficiency. *ACS Nano* **2022**, *16* (6), 9701−9712.
(10) Stam, M.; Almeida, G.; Ubbink, R. F.; van der Poll, L. M.; Vogel, Y. B.; Chen, H.; Giordano, L.; Schiettecatte, P.; Hens, Z.; Houtepen, A. J. Near-Unity Photoluminescence Quantum Yield of Core-Only InP Quantum Dots via a Simple Postsynthetic InF_3 Treatment. *ACS Nano* **2024**, *18* (22), 14685−14695.
(11) Almeida, G.; van der Poll, L.; Evers, W. H.; Szoboszlai, E.; Vonk, S. J. W.; Rabouw, F. T.; Houtepen, A. J. Size-Dependent Optical Properties of InP Colloidal Quantum Dots. *Nano Lett.* **2023**, *23* (18), 8697−8703.
(12) Li, H.; Zhang, W.; Bian, Y.; Ahn, T. K.; Shen, H.; Ji, B. ZnF2-Assisted Synthesis of Highly Luminescent InP/ZnSe/ZnS Quantum Dots for Efficient and Stable Electroluminescence. *Nano Lett.* **2022**, *22* (10), 4067−4073.
(13) Cerpentier, J.; Karadza, B.; van Avermaet, H.; Giordano, L.; Schiettecatte, P.; Hens, Z.; Meuret, Y. InP-based quantum dot on-chip white LEDs with optimal circadian efficiency. *Optics & Laser Technology* **2023**, *167*, 109839.
(14) Karadza, B.; Schiettecatte, P.; Van Avermaet, H.; Mingabudinova, L.; Giordano, L.; Respekta, D.; Deng, Y.-H.; Nakonechnyi, I.; De Nolf, K.; Walravens, W.; Meuret, Y.; Hens, Z. Bridging the Green Gap: Monochromatic InP-Based Quantum-Dot-on-Chip LEDs with over 50% Color Conversion Efficiency. *Nano Lett.* **2023**, *23* (12), 5490−5496.
(15) Walukiewicz, W. Defects and Self-Compensation in Semiconductors. In *Wide-Gap Chalcopyrites*; Siebentritt, S., Rau, U., Eds.; Springer: Berlin, 2006; pp 35−54.
(16) Heinrich, M.; Domke, C.; Ebert, P.; Urban, K. Charged steps on III-V compound semiconductor surfaces. *Phys. Rev. B* **1996**, *53* (16), 10894−10897.
(17) Kabiraj, D.; Grötzschel, R.; Ghosh, S. Modification of charge compensation in semi-insulating semiconductors by high energy light ion irradiation. *J. Appl. Phys.* **2008**, *103* (5), 053703.
(18) du Fossé, I.; ten Brinck, S.; Infante, I.; Houtepen, A. J. Role of Surface Reduction in the Formation of Traps in n-Doped II-VI Semiconductor Nanocrystals: How to Charge without Reducing the Surface. *Chem. Mater.* **2019**, *31* (12), 4575−4583.
(19) du Fossé, I.; Lal, S.; Hossaini, A. N.; Infante, I.; Houtepen, A. J. Effect of Ligands and Solvents on the Stability of Electron Charged CdSe Colloidal Quantum Dots. *J. Phys. Chem. C* **2021**, *125* (43), 23968−23975.
(20) Geuchies, J. J.; Dijkhuizen, R.; Koel, M.; Grimaldi, G.; du Fossé, I.; Evers, W. H.; Hens, Z.; Houtepen, A. J. Zero-Threshold Optical Gain in Electrochemically Doped Nanoplatelets and the Physics behind It. *ACS Nano* **2022**, *16* (11), 18777−18788.
(21) Chen, H.; Ubbink, R. F.; Olsthoorn, R. A.; Stam, M.; t Hoen, J.; Savenije, T. J.; Houtepen, A. J. Potential of Electrochemical Charge Injection for Quantum Dot Light-Emitting Devices. *Chem. Mater.* **2025**, *37* (12), 4435−4444.
(22) van der Stam, W.; Grimaldi, G.; Geuchies, J. J.; Gudjonsdottir, S.; van Uffelen, P. T.; van Overeem, M.; Brynjarsson, B.; Kirkwood, N.; Houtepen, A. J. Electrochemical Modulation of the Photophysics of Surface-Localized Trap States in Core/Shell/(Shell) Quantum Dot Films. *Chem. Mater.* **2019**, *31* (20), 8484−8493.
(23) Pu, C.; Dai, X.; Shu, Y.; Zhu, M.; Deng, Y.; Jin, Y.; Peng, X. Electrochemically-stable ligands bridge the photoluminescence-electroluminescence gap of quantum dots. *Nat. Commun.* **2020**, *11* (1), 937.
(24) Vogel, Y. B.; Pham, L. N.; Stam, M.; Ubbink, R. F.; Coote, M. L.; Houtepen, A. J. Solvation Shifts the Band-Edge Position of Colloidal Quantum Dots by Nearly 1 eV. *J. Am. Chem. Soc.* **2024**, *146* (14), 9928−9938.
(25) Vogel, Y. B.; Stam, M.; Mulder, J. T.; Houtepen, A. J. Long-Range Charge Transport via Redox Ligands in Quantum Dot Assemblies. *ACS Nano* **2022**, *16* (12), 21216−21224.
(26) Guyot-Sionnest, P. Charging colloidal quantum dots by electrochemistry. *Microchimica Acta* **2008**, *160* (3), 309−314.
(27) Gudjonsdottir, S.; Koopman, C.; Houtepen, A. J. Enhancing the stability of the electron density in electrochemically doped ZnO quantum dots. *J. Chem. Phys.* **2019**, *151* (14), 144708.
(28) Gudjonsdottir, S.; van der Stam, W.; Kirkwood, N.; Evers, W. H.; Houtepen, A. J. The Role of Dopant Ions on Charge Injection and Transport in Electrochemically Doped Quantum Dot Films. *J. Am. Chem. Soc.* **2018**, *140* (21), 6582−6590.
(29) Roest, A. L.; Germeau, A.; Kelly, J. J.; Vanmaekelbergh, D.; Allan, G.; Meulenkamp, E. A. Long-Range Transport in an Assembly of ZnO Quantum Dots: The Effects of Quantum Confinement, Coulomb Repulsion and Structural Disorder. *ChemPhysChem* **2003**, *4* (9), 959−966.
(30) Stam, M.; du Fossé, I.; Infante, I.; Houtepen, A. J. Guilty as Charged: The Role of Undercoordinated Indium in Electron-Charged Indium Phosphide Quantum Dots. *ACS Nano* **2023**, *17* (18), 18576−18583.
(31) Yu, W.; Richter, M. H.; Buabthong, P.; Moreno-Hernandez, I. A.; Read, C. G.; Simonoff, E.; Brunschwig, B. S.; Lewis, N. S. Investigations of the stability of etched or platinized p-InP(100) photocathodes for solar-driven hydrogen evolution in acidic or alkaline aqueous electrolytes. *Energy Environ. Sci.* **2021**, *14* (11), 6007−6020.
(32) Park, J.; Kim, T.; Kim, D. Charge Injection and Energy Transfer of Surface-Engineered InP/ZnSe/ZnS Quantum Dots. *Nanomaterials* **2023**, *13* (7), 1159.

(33) Park, J.; Won, Y.-H.; Kim, T.; Jang, E.; Kim, D. Electrochemical Charging Effect on the Optical Properties of InP/ZnSe/ZnS Quantum Dots. *Small* **2020**, *16* (41), 2003542.
(34) Crisp, R. W.; Kirkwood, N.; Grimaldi, G.; Kinge, S.; Siebbeles, L. D. A.; Houtepen, A. J. Highly Photoconductive InP Quantum Dots Films and Solar Cells. *ACS Applied Energy Materials* **2018**, *1* (11), 6569−6576.
(35) Tessier, M. D.; Dupont, D.; De Nolf, K.; De Roo, J.; Hens, Z. Economic and Size-Tunable Synthesis of InP/ZnE (E = S, Se) Colloidal Quantum Dots. *Chem. Mater.* **2015**, *27* (13), 4893−4898.
(36) Giordano, L.; Schiettecatte, P.; Coppel, Y.; Zhao, Q.; Staechelin, Y. U.; Bonifas, G.; Van Avermaet, H.; Nayral, C.; Lange, H.; Vantomme, A.; Delpech, F.; Hens, Z. The Core/Shell Interface in InP/ZnSe Colloidal Quantum Dots. *Chem. Mater.* **2025**, *37* (21), 8724−8732.
(37) Hughes, K. E.; Stein, J. L.; Friedfeld, M. R.; Cossairt, B. M.; Gamelin, D. R. Effects of Surface Chemistry on the Photophysics of Colloidal InP Nanocrystals. *ACS Nano* **2019**, *13* (12), 14198−14207.
(38) Gary, D. C.; Terban, M. W.; Billinge, S. J. L.; Cossairt, B. M. Two-Step Nucleation and Growth of InP Quantum Dots via Magic-Sized Cluster Intermediates. *Chem. Mater.* **2015**, *27* (4), 1432−1441.
(39) Ubbink, R. F.; Almeida, G.; Iziyi, H.; du Fossé, I.; Verkleij, R.; Ganapathy, S.; van Eck, E. R. H.; Houtepen, A. J. A Water-Free In Situ HF Treatment for Ultrabright InP Quantum Dots. *Chem. Mater.* **2022**, *34* (22), 10093−10103.
(40) Janke, E. M.; Williams, N. E.; She, C.; Zherebetskyy, D.; Hudson, M. H.; Wang, L.; Gosztola, D. J.; Schaller, R. D.; Lee, B.; Sun, C.; Engel, G. S.; Talapin, D. V. Origin of Broad Emission Spectra in InP Quantum Dots: Contributions from Structural and Electronic Disorder. *J. Am. Chem. Soc.* **2018**, *140* (46), 15791−15803.
(41) Dümbgen, K. C.; Leemans, J.; De Roo, V.; Minjauw, M.; Detavernier, C.; Hens, Z. Surface Chemistry of InP Quantum Dots, Amine-Halide Co-Passivation, and Binding of Z-Type Ligands. *Chem. Mater.* **2023**, *35* (3), 1037−1046.
(42) Ubbink, R. F.; Vogel, Y. B.; Stam, M.; Chen, H.; Houtepen, A. J. Where Do the Electrons Go? Studying Loss Processes in the Electrochemical Charging of Semiconductor Nanomaterials. *Chem. Mater.* **2025**, *37* (2), 736−745.
(43) van der Stam, W.; du Fossé, I.; Grimaldi, G.; Monchen, J. O. V.; Kirkwood, N.; Houtepen, A. J. Spectroelectrochemical Signatures of Surface Trap Passivation on CdTe Nanocrystals. *Chem. Mater.* **2018**, *30* (21), 8052−8061.
(44) Houtepen, A. J.; Vanmaekelbergh, D. Orbital Occupation in Electron-Charged CdSe Quantum-Dot Solids. *J. Phys. Chem. B* **2005**, *109* (42), 19634−19642.
(45) Franceschetti, A.; Zunger, A. Optical transitions in charged CdSe quantum dots. *Phys. Rev. B* **2000**, *62* (24), R16287−R16290.
(46) Boehme, S. C.; Vanmaekelbergh, D.; Evers, W. H.; Siebbeles, L. D. A.; Houtepen, A. J. In Situ Spectroelectrochemical Determination of Energy Levels and Energy Level Offsets in Quantum-Dot Heterojunctions. *J. Phys. Chem. C* **2016**, *120* (9), 5164−5173.
(47) Allred, A. L. Electronegativity values from thermochemical data. *Journal of Inorganic and Nuclear Chemistry* **1961**, *17* (3), 215−221.
(48) Bard, A. J.; Faulkner, L. R. *Electrochemical Methods: Fundamentals and Applications*, 2nd ed.; Wiley Textbooks, 2001.
(49) Haynes, W. M. *CRC Handbook of Chemistry and Physics*, 95th ed.; CRC Press: Boca Raton, FL, 2014.
(50) Schiettecatte, P.; Giordano, L.; Cruyssaert, B.; Bonifas, G.; De Vlamynck, N.; Van Avermaet, H.; Zhao, Q.; Vantomme, A.; Nayral, C.; Delpech, F.; Hens, Z. Enhanced Surface Passivation of InP/ZnSe Quantum Dots by Zinc Acetate Exposure. *Chem. Mater.* **2024**, *36* (12), 5996−6005.
(51) Gao, Y.; Sandeep, C. S.; Schins, J. M.; Houtepen, A. J.; Siebbeles, L. D. Disorder strongly enhances Auger recombination in conductive quantum-dot solids. *Nat. Commun.* **2013**, *4* (1), 2329.
(52) Dhaene, E.; Billet, J.; Bennett, E.; Van Driessche, I.; De Roo, J. The Trouble with ODE: Polymerization during Nanocrystal Synthesis. *Nano Lett.* **2019**, *19* (10), 7411−7417.
(53) Hendricks, M. P.; Campos, M. P.; Cleveland, G. T.; Jen-La Plante, I.; Owen, J. S. A tunable library of substituted thiourea precursors to metal sulfide nanocrystals. *Science* **2015**, *348* (6240), 1226−1230.
(54) Magde, D.; Wong, R.; Seybold, P. G. Fluorescence Quantum Yields and Their Relation to Lifetimes of Rhodamine 6G and Fluorescein in Nine Solvents: Improved Absolute Standards for Quantum Yields. *Photochem. Photobiol.* **2002**, *75* (4), 327−334.


CAS BIOFINDER DISCOVERY PLATFORM™
CAS BIOFINDER HELPS YOU FIND YOUR NEXT BREAKTHROUGH FASTER
Navigate pathways, targets, and diseases with precision
Explore CAS BioFinder
CAS
A division of the American Chemical Society

https://doi.org/10.1021/acs.chemmater.5c02861
Chem. Mater. 2026, 38, 1407−1414